Inorganic Chemistry Communications 145 (2022) 110017

Contents lists available at ScienceDirect

Inorganic Chemistry Communications

journal homepage: www.elsevier.com/locate/inoche

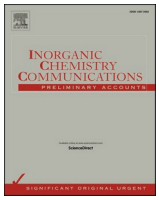

Short communication

Microstructural and optical duality of TiO_2/Cu/TiO_2 trilayer films grown by atomic layer deposition and DC magnetron sputtering

S.S. Fouad [a], Eszter Baradács [b,c], M. Nabil [d,*], Bence Parditka [b], S. Negm [d], Zoltán Erdélyi [b]

[a] Department of Physics, Faculty of Education, Ain Shams University, Cairo 11566, Egypt
[b] Department of Solid State Physics, Faculty of Sciences and Technology, University of Debrecen, P.O. Box 400, H- 4002 Debrecen, Hungary
[c] Department of Environmental Physics, University of Debrecen, H-4026 Debrecen, Poroszlay u. 6, Hungary
[d] Department of Basic Engineering Sciences, Faculty of Engineering (Shoubra), Benha University, Benha, Egypt

ARTICLE INFO

Keywords:
Titanium dioxide
Interlayer
Band gap
Photocatalyst
Optical basicity

ABSTRACT

In this research, we report a comparative study of trilayer TiO_2(60 nm)/Cu/TiO_2(60 nm) thin film as a function of different Cu interlayer thickness (20, 40 and 60 nm), fabricated by atomic layer deposition (ALD) and DC magnetron sputtering. The surface morphology, elemental information and optical properties, were tested as a function of Cu interlayer thickness by scanning electron microscopy (SEM), energy dispersive X-ray spectrometer (EDX) and double beam spectrophotometer (UV–vis) respectively.The growth mechanism and the microstructural conversion were investigated. The absorption spectrum was mesured and used to calculate the energy band gap (E_g). The obtained results show that the increase of the Cu interlayer enhance the activity of photocatalysis by employing distinct modification strategies to decrease the indirect optical band gap energy from 2.85 to 1.86 eV, and conventionally making the photocatalyst efficient to absorb visible light range. The role of the optical energy band gap E_g as well as the average electronegativity (χ) as basic parameters of optical basicity (Λ) and refractive index (n) has been emphasized. Values of electronegativity (χ), phase velocity (V) and transmission coefficient (T_C) decreased, while the refractive index, optical basicity, electronic polarizability (α_e), and reflection loss (R_L) increased with increasing Cu interlayer thickness. A good agreement is observed among the selected parameters. The results demonstrate that the ALD and the DC magnetron sputtering are promising techniques for preparing TiO_2/Cu/TiO_2 thin films, with different thickness of copper (Cu), that can be used in low-cost mid-IR detection and can enhanced the properties of optoelectronic devices.

1. Introduction

Transparent conductive oxides (TCO) are truly remarkable materials for optoelectronic devices, such as solar cell and light–emitting diodes, because of their unique characteristics of low electrical resistivity and high optical transmittance [1–3]. Titanium dioxide is a photosensitive semiconductor, which can only absorb ultraviolet light, because it has wide band gap energy of 3.0 to 3.2 eV that limits its absorption of solar radiation to the UV light range. The photocatalytic activity of TiO_2 is very limited by the rapid recombination of the electron-hole pairs. TiO_2 is a relatively cheap, photochemical, stable, non-toxic material, theses properties make it suitable for multilayer thin film. Several studies have been carried out to reduce the band gap energy and modify the electronic structure of TiO_2 by the insertion or doping non-metal ions, rare earth elements or the addition of transition metals [4–7]. Transitional metal doping had been an effective alternative, in reducing the band gap of TiO_2 and extending its activity to make better use of solar energy. To manipulate the optical and other related parameters of TiO_2 and make it of high interest for applications, the addition of Cu as an Ib group element has been found to be one of the most suitable additives for achieving excellent optical results of TiO_2 films. Recently, multilayer thin films doped with transparent conductive oxide, have received considerable attention because of their potential applications in different devices, some of which are in spintronics and optical filters [8–10]. Theoretical investigations have shown that Cu doping can reduce the band gap of TiO_2 because it creates impurity levels that allow the electronic transition within the conduction and valence band to be reduced [11]. The knowledge of the optical basicity and the polarizability is necessary as it affects the conductivity, refractive index and optical properties that are basic parameters for any application in the

* Corresponding author.
E-mail address: Mohamed.mohamed04@feng.bu.edu.eg (M. Nabil).

https://doi.org/10.1016/j.inoche.2022.110017
Received 22 June 2022; Received in revised form 5 September 2022; Accepted 15 September 2022
Available online 28 September 2022

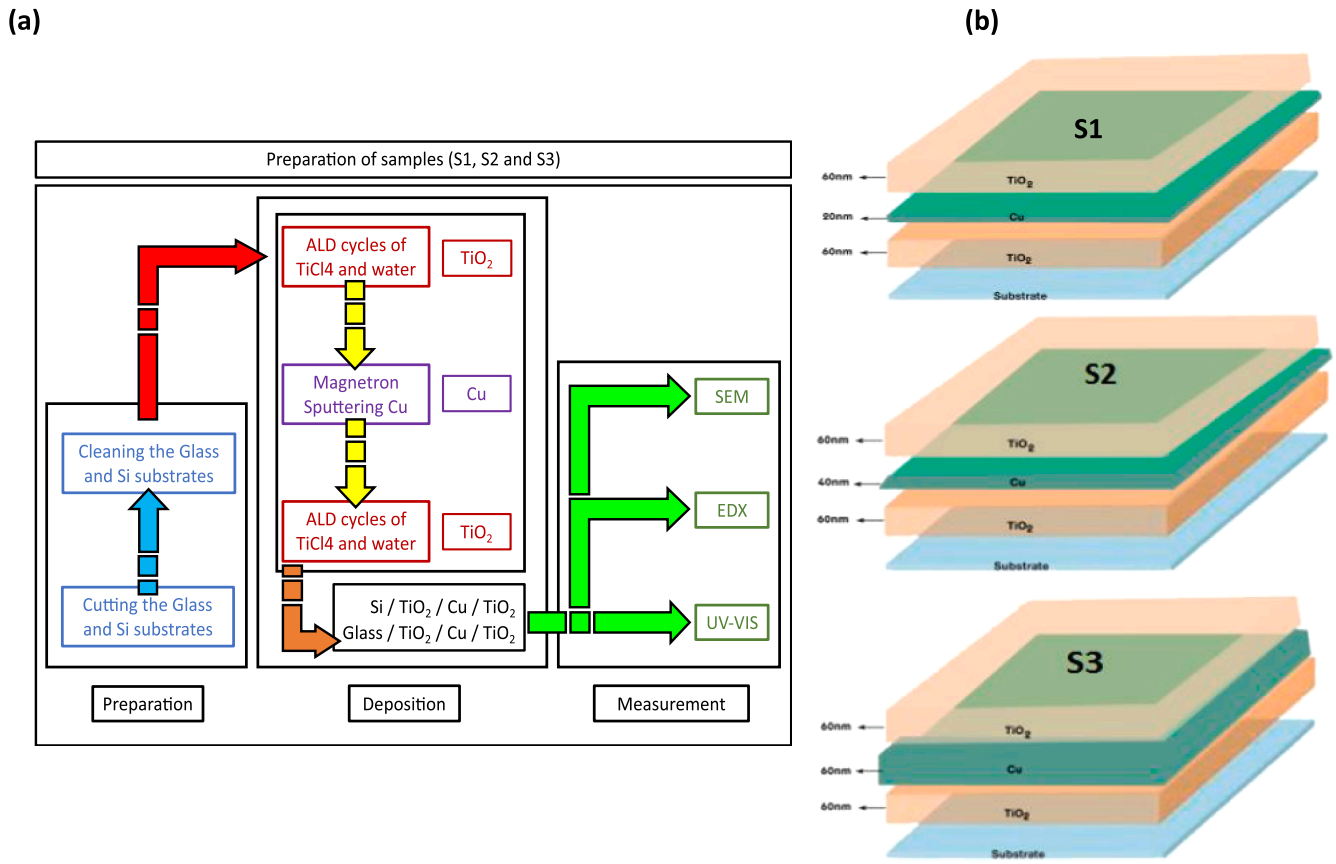

Fig. 1. **(a)** Schematic chart of the depositon process of the samples. **(b)**Schematic of physical models of S1,S2 and S3 trilayer films.

development of communication and information technology [12,13]. Only few papers focused on $TiO_2/Cu/TiO_2$ films by ALD and Magnetron Sputtering have been performed [5–7].The atomic layer deposition (ALD) is more powerful in preparing such multilayers than any other techniques In the present study a high-quality $TiO_2/Cu/TiO_2$ films, with different Cu interlayer thickness are fabricated by (ALD) and magnetron sputtering. The influence of the Cu interlayer on the structural and optical properties and optical basicity were analyzed.

2. Experimental procedure

Trilayer films of $TiO_2/Cu/TiO_2$ with a variety of Cu interlayer thickness were deposited on glass and silicon substrates, The TiO_2 layers were deposited by atomic layer deposition (ALD), whereas the Cu interlayer by magnetron sputtering in a three-step deposition procedure: ALD-Sputtering-ALD. The number of ALD cycles were chosen to obtain an estimated thickness for TiO_2 of 60 nm based on previous tests and profilometer measurements, while Cu interlayers of 20, 40 and 60 nm thickness were grown by magnetron sputtering based upon deposition rate measurements performed under the same conditions as the deposition. The trilayer deposition were performed as follows:

The TiO_2 films were grown on the substrates by atomic layer deposition (ALD) using BeneqTFS-200 type ALD reactor. The pressure was stabilized at 1 and 9 mbar in the reactor and the main chamber, respectively. Titanium tetrachloride ($TiCl_4$) and H_2O precursors (purchased from Epivalence, Cleveland, UK and Sigma-Aldrich/Merc, Hungary respectively) were used for the deposition of the films. The samples were prepared in thermal mode at 108 °C. 700 cycles of TiO_2 were deposited with pulse time of 300 ms for both $TiCl_4$ and H_2O and purge times of 3 s, respectively. The Cu layers were grown by DC magnetron sputtering at room temperature. The base pressure of the sputtering chamber was lower than 5×10^{-7}mbar. During deposition the Ar (99.999 %) (purchased from Linde-Hungary) pressure (under dynamic flow) was 7×10^{-3} mbar. The purity of Cu was 99.99 %.was purchased from Kurt.J.Lesker (EU). The deposition rate was calibrated using Ambios XP-1 profilometer.The research chart schematic of the sample deposition process can be seen in details in Fig. 1 **(a).**

The resulting trilayers are denoted by S1, S2 and S3 as shown in Fig. 1 **(b).** The microstructure and the compositions of the samples were determined by energy dispersive X-ray spectrometer (EDX) connected to the field emission scanning electron microscope (FE-SEM) (QUANTA FEG 250 model). The optical absorption was measured using a V-670 Jasco double-beam spectrophotometer, which utilizes a unique, single monochromator design covering a wavelength range from 190 to 2700 nm.

3. Results and Discussion

3.1. Structure Analysis

A high resolution SEM was used to determine the morphology of the Cu interlayers in $TiO_2/Cu/TiO_2$. The SEM images for S1, S2, and S3 presented in Fig. 2 **(a)** Considering that the three individual FESEM image of Fig. 2(a) share the same magnification,It is clearly visible,even without a detailed image analysis,that Cu interlayer characteristic distribution,or morphology changes significantly from S1 to S3..However SEM images subjected to image processing further supported the idea that the thicker the Cu interlayer is, the large the interconnected granular clusters. FESEM images were subjected to image analysis to clear up morphological differences, from S1to S3 in parallel with an increase amount of Cu on the surface. Clustering is one of the most common exploratory data analysis technique used to get an intuition about the structure ot the data. Therefore, the size of the Cu clusters grains grow in size,and the agglomeration of this interlayer is more pronounced with

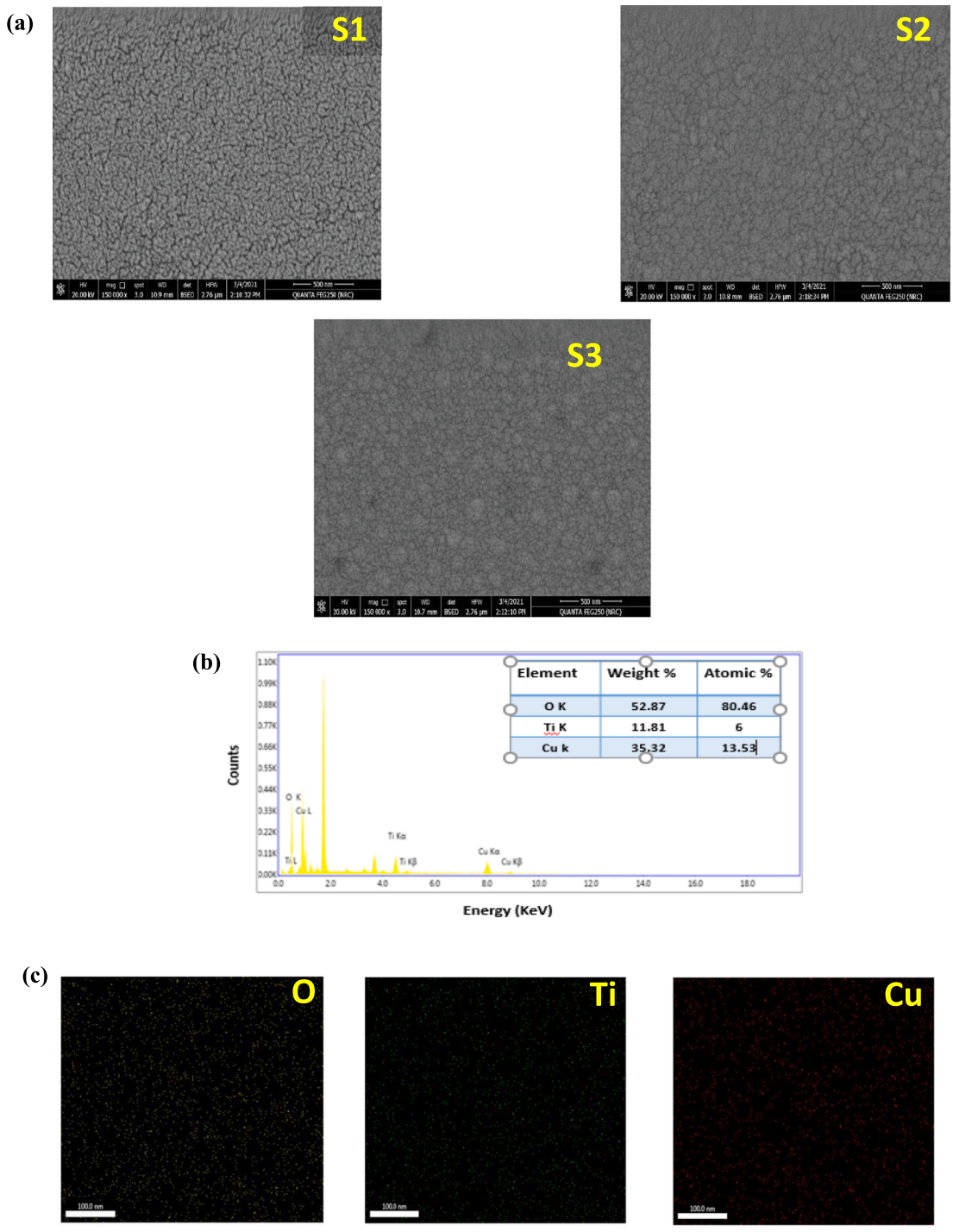

Fig. 2. **(a)** SEM images for TiO_2/Cu/TiO_2 samples S1, S2 and S3. **(b)**EDX spectra of TiO_2/Cu/TiO_2 sample S3. **(c)** The elemental mapping of TiO_2/Cu/TiO_2 samples S3.

Table 1
The number of clusters and the average size of clusters for the studied TiO_2/Cu/TiO_2 films with different Cu thickness.

Samples	No of clusters	Avg. size of clusters (pixels)
S1	273	3728.4
S2	171	6034.5
S3	102	10647.5

each sample. Since our data type is an image so we can use either pixel values or structure in image. As can be seen in Table1, the number of clusters decreases about a factor of 3 and in the same time the aversge size increases accordingly.

As it can be seen, when the thickness of the Cu interlayer increases, the size of the Cu clusters, nanoparticles and their agglomeration increases. This change can be attributed to the change in growth mode, as the Cu surface coverage increases. This is due to the fact that when the number of coating layers increases then the lattice mismatching among the layers were reduced, their for the grain size increases. The obtained results are consistent with those obtained previously [14].

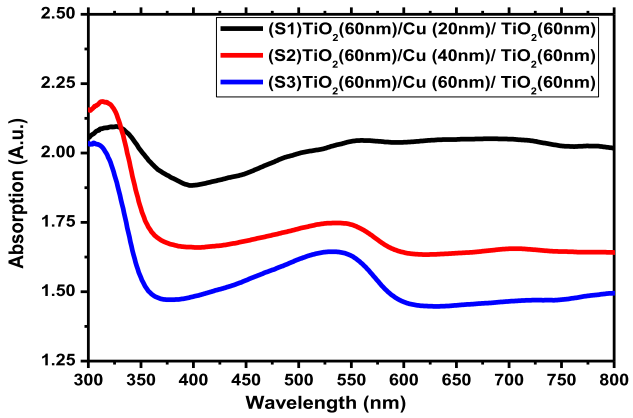

Fig. 3. Absorption band for TiO_2/Cu/TiO_2 samples S1, S2 and S3.

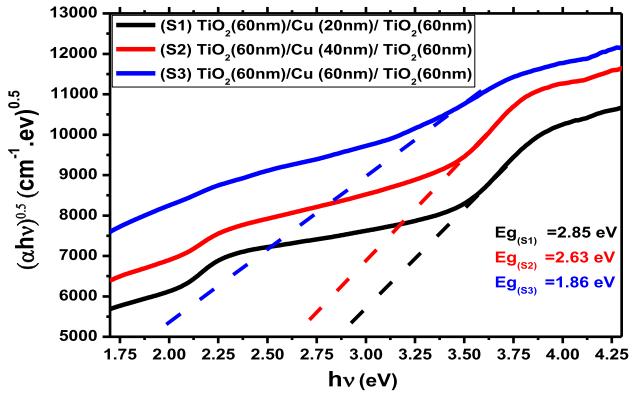

Fig. 4. $(\alpha h\nu)^{0.5}$ versus $(h\nu)$ plot for TiO_2/Cu/TiO_2 for samples S1, S2 and S3.

Next, the clustered Cu layer was coated with TiO_2. Thus the final Cu-"doped" TiO_2 structure was formed. This structure was also analyzed by energy-dispersive X-ray spectroscopy (EDX). The results for sample S3, as a representative example, are shown in Fig. 2**(b)**. The analysis shows insignificant variation in the composition of the as-prepared sample. The elemental mapping of S3 is also presented in Fig. 2**(c)**. As observed in the SEM images, the elemental maps also clearly show that Cu was successfully deposited on the entire surface of the TiO_2 films. For the S3 sample, the nominal Cu thickness is one third of the total sample thickness, which is consistent with the proportion of components found in the EDX analysis.

3.2. Absorption coefficient (α) and optical energy gap (E_g)

According to [15,16] Cu enhance the visible absorption of Cu-TiO_2 in the range of 400–100 nm. In this part of the spectrum,metal free electrons reflectivity is very small and is affected by light absorption from interband electron transition. Fig. 3 shows the optical absorption spectra of S1, S2 and S3 versus the incident wavelength (λ) in the domain (300–800 nm). All the samples have a peak around ≈ 350 nm, which

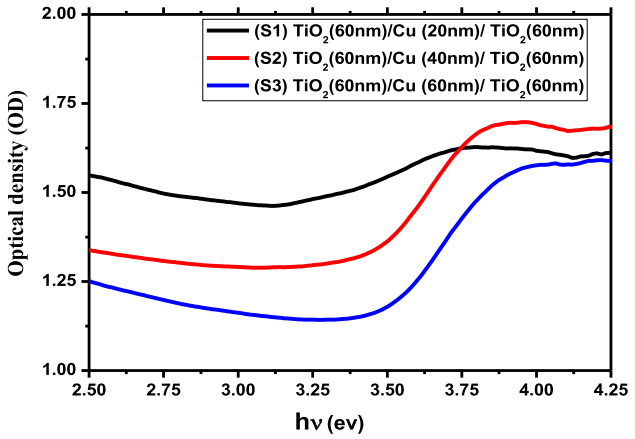

Fig. 5. Optical density versus $(h\nu)$ plot for TiO_2/Cu/TiO_2 samples S1, S2 and S3.

may be attributed to the original band structure of TiO_2. The increase in absorbance seen for S1, S2 and S3 at wavelengths longer than ≈ 400 nm may be attributed to the increase in the thickness of the Cu interlayer that enhance the activity of photocatalytic efficient employing distinct modifications to absorb visible light range. Also as Cu interlayer increases,more bound electrons are available for excitation producing a decrease in the optical absorption spectra. An absorpion decrease with increasing metal interlayer thickness was also observed by [17]. As the thickness of the Cu tinterlayer increases, the valence band can be excited with photons of lower energy than for pure TiO_2 resulting in a decrease in transmission.

Based on the recorded absorption spectra for the three samples, the absorption coefficient ***(α)*** and the optical energy gap ***(E_g)*** were determined. The value of ***(α)*** can be obtained by using the following expression [18]:

$$\boldsymbol{\alpha} = \frac{2.303\boldsymbol{A}}{\boldsymbol{t}} \quad (1)$$

where ***t*** is the film thickness, and ***A*** is the value of the corresponding optical absorbance.

The ***E_g*** optical energy gap could be determined by using the well-known equation as follows [19–21]:

$$\boldsymbol{\alpha h\nu} = \boldsymbol{B}(\boldsymbol{h\nu} - \boldsymbol{E_g})^{\boldsymbol{r}} \quad (2)$$

where ***B*** is a constant denoting the band tail parameter and ***r*** is the power factor that determines the type of the optical transition that may equal to ½ or 2 for direct or indirect allowed transition respectively. The best fit was obtained for indirect optical energy gap were ***r = 2***. Fig. 4 implies the alteration of ***$(\alpha h\nu)^{0.5}$*** versus ***$(h\nu)$*** for S1, S2 and S3. The optical energy band gap values were evaluated by extrapolating the linear portion to photon energy axis ($\alpha h\nu = 0$), as shown in Fig. 4, and presented in Table 2 in comparison with the band gap of pure TiO_2 given in [22]. Thus, the obtained ***E_g*** values decreased from 2.85 eV to 1.86 eV with the increase of Cu interlayer thickness from 20 nm to 60 nm.The total bandgap shift was approximately 0.99 eV. These results suggest

Table 2
The direct optical energy gap **(E_g)**, Average optical electronegativity **($\Delta\chi$)**, Linear reflection index **(n)**, Electronic polarizability (α_e), Optical basicity **(A^0)**, Phase velocity **(v)**.The transmission coefficient **(TC)** and Reflection loss **(R_L)**, for the studied TiO_2/Cu/TiO_2 films with different thickness prepared by the ALD technique.

Samples	E_g	$\Delta\chi$	n		α_e	A^0	$v \times 10^{-8}$	T	R_L
			Equation (5)	Equation (6)					
TiO_2	3.1	0.833	2.466	2.373	3.994	1.40	1.264	0.715	0.165
S1	2.85	0.766	2.549	2.440	4.044	1.415	1.229	0.701	0.174
S2	2.63	0.706	2.630	2.504	4.089	1.429	1.198	0.688	0.184
S3	1.86	0.499	2.978	2.804	4.246	1.476	1.069	0.632	0.224

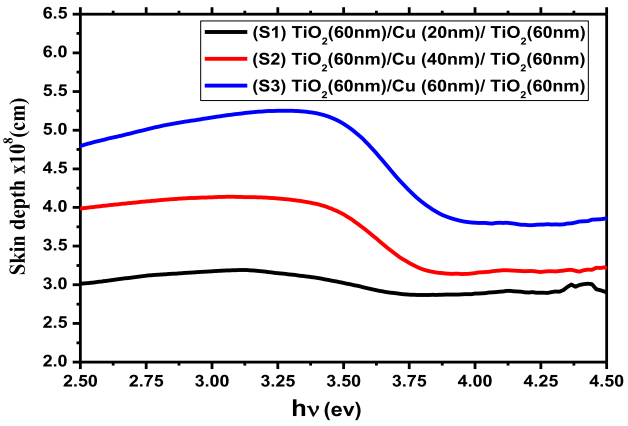

Fig. 6. Skin depth versus the photon energy plot for $TiO_2/Cu/TiO_2$ samples S1, S2 and S3.

that the increase of the thickness of Cu interlayer extend the absorption edge of TiO_2 to visible light and thus enhance the visible absorption in the range 400–1000 nm. The decrease in the band gap is also due to the increase in grain size from (3726.4 to 10647.5 pixels) as seen in Fig. 2 and Table1. This behavior was also observed by [23], were they suggested that some sub- bands can be formed due to defect levels in the forbidden band of TiO_2 thereby reducing the band-gap energy.

On the other hand, optical density ***(OD)*** or absorbance is proportional to the thickness of the samples and their composition. The optical density ***(OD)*** can be calculated by OD = αt, as given in [18]. Fig. 5 depicts the variation of the obtained OD for S1, S2 and S3 with the incident photon energy ***hν*** (eV). As seen the optical density decreases with the increase of the thickness of Cu interlayer.

The skin depth ***(δ)*** is defined as the depth where the current density is just about 37 % of the value at the surface. It depends on the conductivity of the metals: higher the conductivity smaller the skin depth and vice versa. Skin depth matters for lower frequency regimes, such as microwaves. The skin depth or the penetration depth is related to the absorption coefficient by the following simple relation: $\delta = 1/\alpha$ [16]. Fig. 6 shows the dependence of skin depth on the incident photon energy ***(hν)***.

It is clear that the skin depth increases with increasing Cu content and decreases with increasing photon energy.

3.3. Optical basicity.

Optical basicity is related to optical properties. The optical basicity expresses the ability of oxide ions to donate electrons [22]. Optical basicity expresses the basicity of any material in terms of electron density. The theoretical optical basicity of multi-component oxides can be estimated through the average optical electronegativity ***(Δχ)***. The correlation between electronegativity and ionicity is well established in the literature and can be estimated using the relation given by [24].

$$\Delta\chi = 0.2688E_g \tag{3}$$

The correlation proposed by Duffy to calculate the value of optical basicity for oxides based on the optical electronegativity was [25]:

$$A^0 = 1.59 - 0.2279\Delta\chi \tag{4}$$

Table 2 presents the calculated values of the electronegativity and the oxide optical basicity of S1, S2 and S3. As seen the values of the electronegativity decreases from 0.766 to 0.499, while the values of the optical basicity increase from 1.415 to 1.476 with the increase of Cu interlayer thickness from 20 to 60 nm. A good correspondence exists between the optical basicity estimated by the above method and the average electronegativity that can give insight into the nature of the existing bonding.

3.4. Refractive index

The linear refractive index ***(n)*** is a fundamental physical quantity of materials that represents electromagnetic wave propagation and plays an important role in designing optical devices [26]. The linear refractive index of S1, S2 and S3 was calculated from the optical energy band gap ***(E_g)*** values by using the equation [27]:

$$n = \left(6\sqrt{\frac{5}{E_g}} - 2\right)^{\frac{1}{2}} \tag{5}$$

The values of ***n*** are presented in Table 2. An expression given by Duffy is adopted for the evaluation of the refractive index by using the relation [24]:

$$n = -ln(0.102\Delta\chi) \tag{6}$$

The estimated values of ***n*** are also given in Table 2. As can be seen there is good agreement between the estimated values of ***n*** obtained from Eq (5) and Eq (6). It is also observed that the refractive index increases as the thickness of the Cu interlayers increases. The increase in refractive index is related to the increase in density. Moreover, the decrease in optical energy gap with increasing refractive index values is supported by literature data [28]. In the present study, we are interested in intensities and not in the amplitudes, thus for our system,we obtained the phase velocity ***(v)*** as $v = c/n$, where ***c*** is the speed of light and the reflectivity or reflection loss ***(R_L)***, defined as the ratio of the intensity of the beam reflected from the glass surface to the intensity of the beam incident on the glass surface, and is derived from the following expression [19,29]:

$$R_L = \left(\frac{n-1}{n+1}\right)^2 \tag{7}$$

Table 2 presents the values of ***v*** and R_L for S1, S2 and S3. As can be seen the phase velocity decreases while the reflection loss increases with the increase of Cu interlayer thickness. The transmission coefficient ***(T_C)*** can be estimated by using the following equation [30].

$$T_c = \frac{2n}{n^2+1} \tag{8}$$

The decrease in the transmission coefficient ***Tc*** with the increase of Cu interlayer thickness presented in Table 2, is in a good agreement with the experimentally obtained values of the optical density given in Fig. 5. The relationship between the reflection loss and the transmission coefficient shows a partial inverse proportionality between the two quantities, which is in a good agreement with [16,31]. Another important optical property is the electronic polarizability ***(α_e)***. The electronic polarizability is closely related to numerous properties of the materials, such as conductivity, optical basicity along with the refractive index. The electronic polarizability can be calculated from the refractive index by the relation [19,24,32].

$$\alpha_e = 4.624 - 0.7569\Delta\chi \tag{9}$$

The values of the electronic polarizability for S1, S2 and S3 are given in Table 2. An increase in the value of electronic polarizability with the increase of Cu interlayer is observed. In the present study a good agreement can be observed between the optical basicity, linear refractive index and the electronic polarizability values.

3.5. Optical and electrical conductivity

The optical conductivity ***(σ_{opt})***, and the electrical conductivity ***(σ_e)***, depend upon several parameters, such as the absorption coefficient, the optical band gap and the refractive index. The optical and electrical conductivities of the $TiO_2/Cu/TiO_2$ of different Cu interlayer thicknesses, were determined via the following expressions [18,31–34].

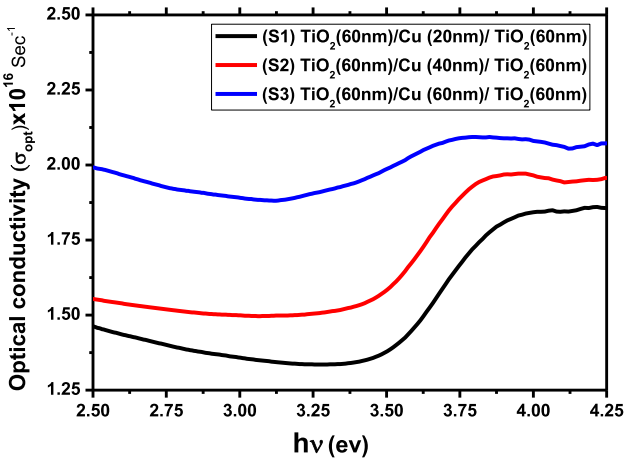

Fig. 7. Optical conductivity versus (hν) plot for TiO_2/Cu/TiO_2 samples S1, S2 and S3.

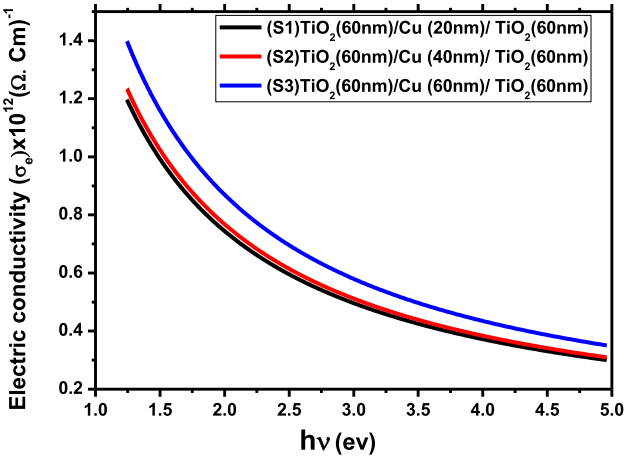

Fig. 8. Electric conductivity versus (hν) plot for TiO_2/Cu/TiO_2 samples S1, S2 and S3.

$$\sigma_{opt} = \frac{\alpha n c}{4\pi} \tag{10}$$

$$\sigma_e = \frac{2\lambda\sigma_{opt}}{\alpha} \tag{11}$$

The subordination of the optical conductivity and electrical conductivity on the variation in photon energy for S1, S2 and S3 are depicted in Fig. 7 and Fig. 8.

The optical conductivity values first decrease and then increase with the increase of the photon energy. This increase is due to the high absorbent nature of the films under study and it also might be due to the photon induced excitation of electrons. On the other hand, the optical and electrical conductivities increase while the optical energy gap ***(E_g)*** decreases, with the increasing of the Cu interlayer thickness. Generally the optical energy gap ***(E_g)*** is directly linked to the conductivity were the electrical conductivity is inversely proportional to the optical energy gap.The above relation is confirmed when comparing the values of the optical energy gap given in Table 2 with the behaviour of the optical and electrical conductivity given in Fig. 7 and Fig. 8.

4. Conclusion

The proposed methodology of TiO_2/Cu/TiO_2 trilayer film synthesis with different Cu interlayer thickness using ALD and magnetron sputtering proved to be very effective. We studied how the thickness of the Cu interlayer affects the structure and optical properties. A precise study has been performed to verify that the introduction of Cu decreases the optical band gap ***(E_g)***, the electronegativity, the phase velocity and the transmission coefficient, while the refractive index, the electronic polarizability, the optical basicity and the reflection loss increase. With increasing Cu content, the bandgap of 2.85 eV decreased down to 1.86 eV, which led to a shift of the absorption edge towards lower energy regions. This may provide significantly more favorable optical applications than pure TiO_2 alone.

Declaration of Competing Interest

The authors declare that they have no known competing financial interests or personal relationships that could have appeared to influence the work reported in this paper.

Data availability

No data was used for the research described in the article.

Acknowledgement.

The samples used in this study were prepared at Debrecen University, Hungary according to the agreement between Faculty of Education, Ain Shams University *"Coordinator and Supervisor Prof.Dr.Suzan Fouad"* and Faculty of Science and Technology ,University of Debrecen *"Coordinator and Supervisor Prof.Dr,Zoltán Erdélyi"* . The samples were measured at Laser Physics and Nanotechnology Unit (LPTU), Faculty of Engineering, Shoubra, Benha University. The research was supported by the Thematic Excellence Programmed (TKP2020-IKA-04) of the Ministry for Innovation and Technology in Hungary.

References

[1] Hanaa Zaka, S.S. Fouad, B. Parditka, A.E. Bekheet, H.E. Atyia, M. Medhat, Z. Erdelyi, Enhancement of dispersion optical parameters of Al_2O_3/ZnO thin films fabricated by ALD, Solar Energy 205 (2020) 79–87.
[2] Das, Himadri Sekhar, Gourisankar Roymahapatra, Prasanta Kumar Nandi, and Rajesh Das, Study the Effect of ZnO/Cu/ZnO Multilayer Structure by Radio Frequency Magnetron Sputtering for Flexible Display Applications, (2021).
[3] Shahid. Hussain, , Xiaoyong Yang, Muhammad Kashif Aslam, Asma Shaheen, Muhammad Sufyan Javed, Nimra Aslam, Bilal Aslam, Guiwu Liu, and Guanjun Qiao, Robust TiN nanoparticles polysulfide anchor for Li–S storage and diffusion pathways using first principle calculations, Chem. Eng. J. 391 (2020) 123595.
[4] H. Elshimy, T. Abdallah, The effect of mechanically milled lead iodide powder on perovskite film morphology, Appl. Phys. A 128 (1) (2022) 1–14.
[5] I. Arora, H. Chawla, A. Chandra, S. Sagadevan, S. Garg, Advances in the strategies for enhancing the photocatalytic activity of TiO_2: Conversion from UV-light active to visible-light active photocatalyst, Inorg. Chem. Commun. 109700 (2022).
[6] Landolsi, Zoubaida, Ibtissem ben Assaker, Daniela Nunes, Abdullah YA Alzahrani, Sherif MAS Keshk, and Radhouane Chtourou, Synthesis and characterization of porous TiO_2 film decorated with bilayer hematite thin film for effective photocatalytic activity, Inorganic Chem. Commun. (2022): 109865.
[7] M. Baruah, S.L. Ezung, S. Sharma, U.B. Sinha, D. Sinha, Synthesis and characterization of Ni-doped TiO_2 activated carbon nanocomposite for the photocatalytic degradation of Anthracene, Inorg. Chem. Commun. (2022), 109905.
[8] H.A. Ahmed, S.I. Abu-Eishah, A.I. Ayesh, S.T. Mahmoud, Synthesis and characterization of Cu-doped TiO_2 thin films produced by the inert gas condensation technique, In J. Phys.: Conference Series, vol. 869, no. 1, p. 012027. *IOP Publishing*, **(2017)**.
[9] E.T. Wahyuni, P.Y. Yulikayani, N.A. Aprilita, Enhancement of visible-light photocatalytic activity of Cu-doped TiO_2 for photodegradation of amoxicillin in water, J. Mater. Environ. Sci 11 (4) (2020) 670–683.
[10] V. Dimitrov, T. Komatsu, An interpretation of optical properties of oxides and oxide glasses in terms of the electronic ion polarizability and average single bond strength, J. Univ. Chem. Technol. Metall 45 (3) (2010) 219–250.
[11] J. Peng, C. Hao, H. Liu, Y. Yan, Transparent TiO2/Cu/TiO2 multilayer for electrothermal application, Materials 14 (4) (2021) 1024.
[12] D.M. Tobaldi, A. Sever Škapin, R.C. Pullar, M.P. Seabra, J.A. Labrincha, Titanium dioxide modified with transition metals and rare earth elements: phase composition, optical properties, and photocatalytic activity, Ceram. Int. 39 (3) (2013) 2619–2629.
[13] Díaz-Uribe, Carlos Enrique, William Andrés Vallejo Lozada, and Fernando Martínez Ortega. "Synthesis and characterization of TiO_2 thin films doped with copper to be used in photocatalysis." Iteckne 10, no. 1 **(2013)**: 16-20.

[14] R. Vidhya, R. Gandhimathi, M. Sankareswari, P. Malliga, J. Jeya, K. Neivasagam, Synthesis and Characterization of Cu Doped TiO_2 Thin Films to Protect Agriculturally Beneficial Rhizobium and Phosphobacteria from UV Light, J. Nanostruct. 8 (3) (2018) 232–241.
[15] R.J. Álvaro, N.D. Diana, A.M. María, Effect of Cu on Optical Properties of TiO_2 Nanoparticles, Contemp. Eng. Sci. 10 (2017) 1539–1549.
[16] Y. Chen, Q. Tao, F.u. Wuyou, H. Yang, Synthesis of PbS/Ni_2+ doped CdS quantum dots cosensitized solar cells: Enhanced power conversion efficiency and durability, Electrochim. Acta 173 (2015) 812–818.
[17] Khan, M. I., K. A. Bhatti, Rabia Qindeel, Hayat Saeed Althobaiti, and Norah Alonizan. "Structural, electrical and optical properties of multilayer TiO_2 thin films deposited by sol–gel spin coating, Results Phys. 7 (2017) 1437-1439.
[18] M. Nabil, S.A. Mohamed, K. Easawi, S.SA. Obayya, S. Negm, H. Talaat, M.K. El-Mansy, Surface modification of CdSe nanocrystals: Application to polymer solar cell, Curr. Appl Phys. 20 (3) (2020) 470–476.
[19] S. Fouad,. S.B. Parditka, A.E. Bekheet, H.E. Atyia, Z. Erdélyi, ALD of TiO_2/ZnO mutilayers towards the understanding of optical properties and polarizability, Opt. Laser Technol. 140 (2021) 107035.
[20] H. Zaka, B. Parditka, Z. Erdélyi, H.E. Atyia, P. Sharma, S.S. Fouad, Investigation of dispersion parameters, dielectric properties and opto–electrical parameters of ZnO thin film grown by ALD, Optik 203 (2020), 163933.
[21] I.M. El Radaf, S.S. Fouad, A.M. Ismail, G.B. Sakr, Influence of Spray time on the optical and electrical properties of $CoNi_2S_4$ thin films, Mater. Res. Express5, 4 (2018), 046406.
[22] Del Angel, Raquel, Juan C. Durán-Álvarez, Rodolfo Zanella, TiO_2-Low Band Gap Semiconductor Heterostructures for Water Treatment Using Sunlight-Driven Photocatalysis" Titanium Dioxide: Material for a Sustainable Environment (2018): 305.
[23] H.-T. Sun, X.-P. Wang, Z.-Q. Kou, L.-J. Wang, J.-Y. Wang, Y.-Q. Sun, Optimization of TiO_2/Cu/TiO_2 multilayers as a transparent composite electrode deposited by electron-beam evaporation at room temperature, Chin. Phys. B 24 (4) (2015), 047701.
[24] J.A. Duffy, Trends in energy gaps of binary compounds: an approach based upon electron transfer parameters from optical spectroscopy, J. Phys. C: Solid State Phys. 13 (16) (1980) 2979.
[25] J.A. Duffy, M.D. Ingram, Comments on the application of optical basicity to glass, J. Non-crystalline Solids 144 (1992) 76–80.
[26] R.R. Reddy, Y. Nazeer Ahammed, P. Abdul Azeem, K. Rama Gopal, T.V.R. Rao, Electronic polarizability and optical basicity properties of oxide glasses through average electronegativity, J. Non-Cryst. Solids 286 (3) (2001) 169–180.
[27] S.S. Fouad, B. Parditka, M. Nabil, E. Baradács, S. Negm, H.E. Atyia, Z. Erdélyi, Bilayer number driven changes in polarizability and optical property in ZnO/TiO_2 nanocomposite films prepared by ALD, Optik 166617 (2021).
[28] C. Ban, M. Xie, X. Sun, J.J. Travis, G. Wang, H. Sun, A.C. Dillon, J. Lian, S. M. George, Atomic layer deposition of amorphous TiO_2 on graphene as an anode for Li-ion batteries, Nanotechnology 24 (42) (2013), 424002.
[29] E.G. El-Metwally, E.M. Assim, S.S. Fouad, Optical characteristics and dispersion parameters of thermally evaporated $Ge_{50}In_4Ga13Se_{33}$ chalcogenide thin films, Opt. Laser Technol. 131 (2020), 106462.
[30] S.S. Fouad, I.M. El Radaf, P. Sharma, M.S. El-Bana, Multifunctional CZTS thin films: structural, optoelectrical, electrical and photovoltaic properties, J. Alloy. Compd. 757 (2018) 124–133.
[31] M. Nabil, F. Horia, S.S. Fouad, S. Negm, Impact of Au nanoparticles on the thermophysicalparameters of Fe_3O_4 nanoparticles for seawater desalination, Opt. Mater. 128 (2022), 112456.
[32] S.S.Fouad, Bence Parditka, M. Nabil, Eszter Baradács, S. Negm, Zoltán Erdélyi, Effect of Cu Interlayer on Opto-Electrical Parameters of Zno Thin Films, J. Mater. Sci.: Mater. Electronics (2022) Accepted.
[33] I.M. El Radaf, H.Y.S. Al-Zahrani, S.S. Fouad, M.S. El-Bana, Profound optical analysis for novel amorphous Cu_2FeSnS_4 thin films as an absorber layer for thin film solar cells, Ceram. Int. 46 (11) (2020) 18778–18784.
[34] M.S. El-Bana, S.S. Fouad, Optoelectrical properties of $Ge_{10}Se_{90}$ and $Ge_{10}Se_{85}Cu_5$ thin films illuminated by laser beams, Appl. Phys. A 124 (2) (2018) 1–8.